BEAM QUALITY STUDIES ON RIKEN RING CYCLOTRON AND RI BEAM FACTORY

N. Fukunishi*, A. Goto, O. Kamigaito, M. Kase, H. Okuno, H. Ryuto, N. Sakamoto, M. Wakasugi, Y. Yano, Cyclotron Center, RIKEN, Saitama, Japan
R. Taki, School of High Energy Accelerator Science, SOKENDAI, Tsukuba, Japan
H. Okamura, CYRIC, Tohoku University, Sendai, Japan

Abstract

The RIKEN RI Beam Factory (RIBF) plans to produce heavy-ion beams of 350 MeV/nucleon over the whole range of atomic masses. An accelerator complex used in the RIBF consists of an existing linear accelerator and five cyclotrons. The RIKEN Ring Cyclotron (RRC), the main accelerator in the present facility, will be an injector of the RIBF. Hence, the beam quality studies on the RRC are indispensable for successful operations of the RIBF. We measured the longitudinal emittance for various beams accelerated by the RRC using a high-resolution magnetic spectrometer SMART. The energy spread and time spread measured for a 95-MeV/nucleon ^{40}Ar beam were 0.13 % (FWHM) and 700 ps (FWHM), respectively. We also estimated phase space distributions of beams of the RIBF at every stage of the acceleration scheme based on the measured emittance. We confirm that our accelerator complex is able to produce heavy-ion beams without any serious beam loss under careful tunings of the accelerators. The beam quality expected in the RIBF is fairly good, at least in the low-beam-intensity region where space-charge effects are not dominant.

ACCELERATION SCHEME IN RIBF

The RIKEN RI Beam Factory [1] is an upgrade project of the present RIKEN Accelerator Research Facility (RARF) and aims to produce the world's most intense RI beams. The accelerators of the present facility are the RIKEN Linear Accelerator (RILAC), an AVF-type cyclotron (AVF) and the RIKEN Ring Cyclotron (RRC). The RILAC and the AVF not only inject beams into the RRC but also provide beams to their own experimental courses. In addition to the existing three accelerators, three new ring cyclotrons are under construction in the RIBF project. The first is a fixed-frequency Ring Cyclotron (fRC) [2], the second is named as the Intermediate-stage Ring Cyclotron (IRC) [3] and the last is the world's first separate-sector type Superconducting Ring Cyclotron (SRC) [4]. The following three acceleration modes will be available in the RIBF. The first uses five accelerators in a series including the RILAC, the RRC, the fRC, the IRC and the SRC. In this mode, all the elements from hydrogen to uranium will be accelerated up to 350 MeV/nucleon. However, the beam energy is fixed because the fRC is a fixed-frequency machine. The second is a variable-energy mode including four frequency-variable accelerators, i.e., the RILAC, the RRC, the IRC and the SRC. This acceleration mode is able to produce, for example, a 400-MeV/nucleon ^{40}Ca beam and a 350-MeV/nucleon ^{86}Kr beam. The last mode aims to produce an 880-MeV polarized deuteron beam. The accelerators employed in the last mode are the AVF, the RRC and the SRC. As explained above, the RRC is a unique injector of the RIBF and studies on its beam qualities are indispensable for successful operations of the RIBF.

*fukunisi@rarfaxp.riken.jp

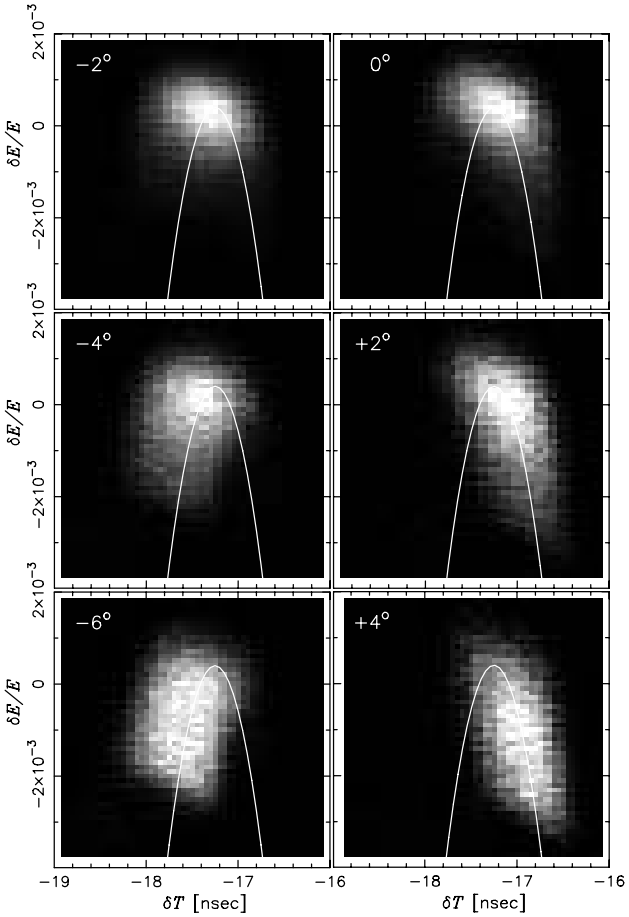

Fig.1 Longitudinal phase space distributions measured for the 95-MeV/nucleon ^{40}Ar beam at the extraction point of the RRC. The vertical axis shows the relative deviation of the kinetic energy (E). The horizontal axis shows the time when particles were extracted from the RRC. The phase of the RF system was displaced from -6 degrees to +4 degrees as shown above.

LONGITUDINAL EMITTANCE MEASUREMENTS

A series of longitudinal emittance measurements were performed using a high-resolution QQDQD-type magnetic spectrometer SMART [5] placed in the E4 experimental vault in the RARF. Ions accelerated by the RRC were guided to the target position of the SMART through a beam transport system including a beam-swinger. Ions were elastically scattered by a 0.25 μm-thick gold-foil target to suppress a counting rate. A scattering angle was chosen to be 2 degrees by using the beam-swinger system. Ions elastically scattered by the target were collimated by a tantalum collimator and colleted on the second focal plane of the SMART (F2), where two plastic scintillators and a position-sensitive silicon detector analyzed the timing and the position of ions. The momentum dispersion was set to be 7.5 meters at the SMART F2. Hereafter, we will report the case of a 95 MeV/nucleon ^{40}Ar beam as an example of the single-turn extraction operation of the RRC. The time resolution was 106 ps (FWHM) and the energy resolution was 2.2×10^{-4} (FWHM) for the ^{40}Ar beam. The details of the measurements are shown in Ref. [6].

Longitudinal emittance of 95MeV/u-^{40}Ar beam

The experiment was performed June 26th, 2003. Measured longitudinal phase space distributions are shown in Fig. 1. We displaced the phase of the RF acceleration system from -6 degrees to +4 degrees. A quadratic correlation between the RF phase and the beam energy was clearly seen. It comes from the fact that the RRC acceleration system has no flat-topping acceleration cavity. The energy spread and the time spread of the beam were determined to be 1.3×10^{-3} (FWHM) and 700 ps (FWHM), respectively.

Comparison with simulation

The longitudinal phase space distributions obtained in the experiments were compared with numerical simulations. The momentum spread and the phase width at the injection point of the RRC was chosen to be 0.3 % (FWHM) and ± 9 degrees (2σ), respectively. The energy spread adopted here is a typical value as reported in the Ref. [7]. The phase width was determined to reproduce the measured time spread for the ^{40}Ar at the extraction of the RRC. Figure 2(a) illustrates the longitudinal phase space distribution given by the present simulation. The injection phase of the beam was optimized in the simulation to obtain the best quality. The result shown in Fig. 2(a) corresponds to the 0 or -2 degree cases of the experiments. Note that the distribution shown in Fig. 2(a) does not include the experimental uncertainties. To make direct comparison with the experiments, we first transformed it into the distribution at the SMART F2 using the effective drift length in which path length differences of ions with different momenta were taken into account. Experimental uncertainties were included there and finally the distribution at the extraction point of the RRC including experimental uncertainties was obtained by applying the transformation from the SMART F2 to the RRC. The result is shown in Fig. 2(b). The cosine-wave shape, which is not seen in the experimental results, becomes unclear but still remains. One possible explanation for the discrepancy is that the momentum spread at the injection of the RRC was much larger than the present assumption. To understand the discrepancy, we need further investigations.

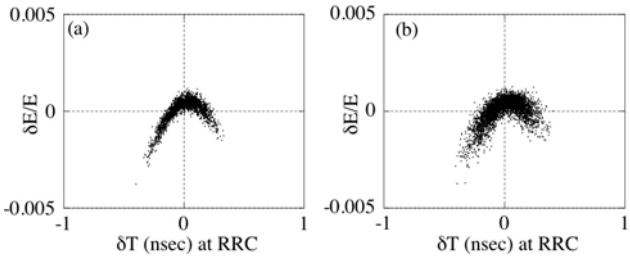

Fig.2 Longitudinal phase space distributions estimated at the extraction point of the RRC with (a) and without (b) experimental uncertainties.

BEAM QUALITY ESTIMATED FOR RIBF

Longitudinal phase space distributions were estimated at every stage of the RIBF from the extraction point of the RRC to the injection point of the SRC. Simulations performed here were based on the measured longitudinal emittance of the 95 MeV/nucleon ^{40}Ar beam. A transverse emittance at the injection point of the RRC was chosen to be 16 π mm mrad. Results shown here do not include following effects. We neglected imperfection of isochronous fields, instabilities of power supplies of magnets, instabilities of RF acceleration systems and other effects originated from poor tunings on an injection energy matching, a dispersion matching and a transverse emittance matching in injecting a beam to the cyclotrons. Within these effects, poor tunings of accelerators give larger effects. We investigated these effects and found that they did not give serious damages on beam qualities under usual tuning of accelerators. We did not also include the space-charge effects in these simulations. The space-charge effects become serious, for example, in the case of a 350-MeV/nucleon 1 pμA $^{238}U^{88+}$ beam as reported in Ref. [8]. Hence, the present results holds for the low-intensity (< 0.1 pμA) region.

^{86}Kr in RILAC + RRC + IRC + SRC mode

Ions extracted from the RRC will be directly injected into the IRC that is 114 meters away from the RRC. The long drift space between the RRC and the IRC expands a beam bunch seriously. However, the IRC, which has flat-topping acceleration system, can accept almost all the ions transferred to the IRC without a rebuncher. The longitudinal phase space distribution at the injection point of the SRC is shown in Fig. 3. The longitudinal emittance is sufficiently small compared with the longitudinal phase space acceptance of the SRC shown by the box in Fig. 3. High quality beams are expected after acceleration of the SRC.

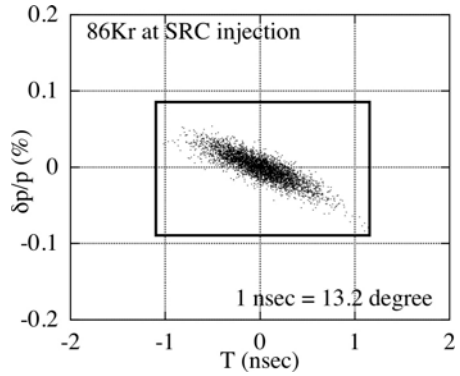

Fig.3 Longitudinal phase space distribution at the injection point the SRC for an ^{86}Kr beam accelerated in the RILAC+RRC+IRC+SRC mode. The box shows the acceptance of the SRC.

^{136}Xe in RILAC + RRC + fRC + IRC + SRC mode

In this mode, ions accelerated by the RRC will be transferred to the fRC through a beam rebuncher planned in the RIBF and further accelerated by the remaining three cyclotrons. As shown in Fig.4, a beam rebuncher between the RRC and the fRC is essential because the operating frequency of the RF system of the fRC is chosen to be three times of the operating frequency of the RRC. The fRC cannot accept beams well accelerated by the RRC without a rebuncher.

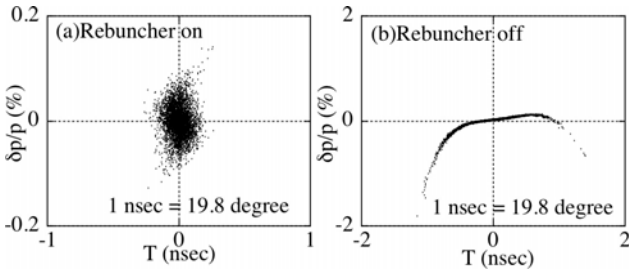

Fig.4 Longitudinal phase space distribution at the extraction point of the fRC with (a) and without (b) a rebuncher.

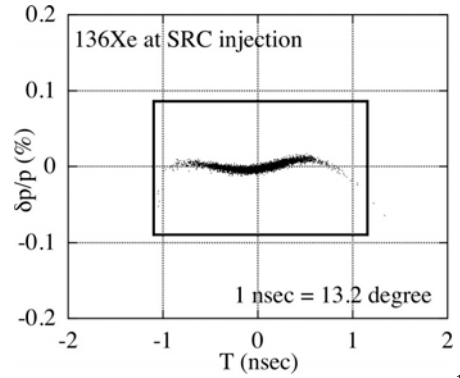

Fig.5 Longitudinal phase space distribution for ^{136}Xe in the RILAC+RRC+fRC+IRC+SRC mode. A box in the figure shows the acceptance.

The distance from the fRC and the IRC is more than 140 meters and we should widen the phase acceptance of the IRC to 30 degrees, by increasing the operating voltage of the flat-topping cavity. The phase space distribution expected at the injection point of the SRC is also shown in Fig.5 with the SRC acceptance. We also expect fairly good beam qualities because the emittance given by the simulation is very small compared with the acceptance.

SUMMARY

We measured longitudinal emittance of the beams accelerated by the RRC to obtain the basic information in estimating the beam qualities of the RIBF. The energy spread and time spread for the ^{40}Ar beam was 0.13% (FWHM) and 700 ps (FWHM), respectively. A series of numerical simulations shows that the beam quality produced by the RRC is good enough to obtain high quality beams in the RIBF.

REFERENCES

[1] Y. Yano *et al.*, in this proceeding.
[2] N. Inabe *et al.*, in this proceeding. T. Mitsumoto et al, in this proceeding.
[3] J. Ohnishi *et al.*, in this proceeding.
[4] H. Okuno *et al.*, in this proceeding.
[5] T. Ichihara *et al.*, Nucl. Phys. A 569 (1994) 287c.
[6] R. Taki, Development of HPGe Detector for the Longitudinal Emittance Measurements, Master thesis of Michigan State University, 2003.
[7] S. Kohara, A. Goto, N. Sakamoto, O. Kamigaito, S. Watanabe, T. Teranishi, T. Katayama, Y. Chiba, M. Kase and Y. Yano, Nucl. Instrm. Meth in Phy. Res. A 526 (2004) p. 230.
[8] S.B. Vorojtsov, A. S. Vorozhtsov, T. Mitsumoto, A. Goto and Y. Yano, Beam Space Charge Simulation in RIKEN SRC, RIKEN-AF-AC-36.